JOURNAL OF VIROLOGY, July 1997, p. 5549–5559 Vol. 71, No. 7
0022-538X/97/$04.00+0

Mutagenesis Analysis of the Murine Leukemia Virus Matrix Protein: Identification of Regions Important for Membrane Localization and Intracellular Transport

YUKO SONEOKA, SUSAN M. KINGSMAN, AND ALAN J. KINGSMAN*

Retrovirus Molecular Biology Group, Department of Biochemistry, University of Oxford, Oxford OX1 3QU, United Kingdom

Received 27 November 1996/Accepted 2 April 1997

We have created two sets of substitution mutations in the Moloney murine leukemia virus (Mo-MuLV) matrix protein in order to identify domains involved in association with the plasma membrane and in incorporation of the viral envelope glycoproteins into virus particles. The first set of mutations was targeted at putative membrane-associating regions similar to those of the human immunodeficiency virus type 1 matrix protein, which include a polybasic region at the N terminus of the Mo-MuLV matrix protein and two regions predicted to form beta strands. The second set of mutations was created within hydrophobic residues to test for the production of virus particles lacking envelope proteins, with the speculation of an involvement of the membrane-spanning region of the envelope protein in incorporation into virus particles. We have found that mutation of the N-terminal polybasic region redirected virus assembly to the cytoplasm, and we show that tryptophan residues may also play a significant role in the intracellular transport of the matrix protein. In total, 21 mutants of the Mo-MuLV matrix protein were produced, but we did not observe any mutant virus particles lacking the envelope glycoproteins, suggesting that a direct interaction between the Mo-MuLV matrix protein and envelope proteins either may not exist or may occur through multiple redundant interactions.

The retroviral *gag* gene product directs virus assembly and the release of virus particles from cell membranes (16, 44). The murine leukemia virus (MuLV) *gag* gene product is a polyprotein precursor, $Pr65^{gag}$, which is translated in the cytoplasm and cleaved during maturation by the viral protease to produce the matrix protein (MA), a protein of unknown function (p12), the capsid protein (CA), and the nucleocapsid protein (NC). The matrix protein is found at the N terminus of $Pr65^{gag}$ and undergoes cotranslational myristylation at the second glycine residue after the removal of the first methionine residue (33). This region probably becomes embedded into the lipid bilayer and plays a significant role in directing the polyprotein precursor to the plasma membrane, the site of virus assembly and budding of virus particles. However, studies using myristylated peptides (27) and proteins (20, 40) show that the 14-carbon saturated fatty acid chain provides barely enough energy to attach a protein to the lipid bilayer membrane. Indeed, two single amino acid changes within the Mason-Pfeizer monkey virus matrix protein were shown to hinder transport to the membrane, despite normal myristylation (34). Moreover, three retroviruses, i.e., avian leukosis virus, visna virus, and equine infectious anemia virus, are not modified by myristic acid but are still transported to the plasma membrane and can effect budding (37). Additional factors, other than myristate, have been shown to increase membrane-binding energy. For example, increases in hydrophobicity by palmitylation of cysteine residues (25, 43) and specific protein-protein interactions (1) provide the additional energy required for anchoring some myristylated proteins to the membrane. Electrostatic interaction of a cluster of basic residues with the acidic phospholipids of the plasma membrane has also been shown to contribute to membrane-binding energy in an additive manner with myristylation for a number of myristylated proteins (reviewed in reference 24). In human immunodeficiency virus type 1 (HIV-1), a polybasic sequence located at the N-terminal region of the matrix protein has been shown to form electrostatic interactions with the acidic phospholipids of the plasma membrane (42, 47). The three-dimensional structure of the HIV-1 matrix protein determined by nuclear magnetic resonance has revealed that these basic residues lie in a beta sheet, which may form below the plasma membrane to interact with the acidic phospholipids (22, 23). Similar basic residues of the simian immunodeficiency virus matrix protein have also been shown to affect particle assembly (11) and lie in a loop which projects outward from the three-dimensional structure, to interact possibly with the phospholipids of the plasma membrane (32). Although the Moloney MuLV (Mo-MuLV) matrix protein has no sequence homology to the HIV-1 or simian immunodeficiency virus matrix protein, it has a similar cluster of basic residues at the N-terminal region of the protein, but the involvement of this cluster in electrostatic interactions and membrane binding has not yet been determined.

The close spatial association of the matrix protein with the membrane has also implicated the matrix protein in forming a specific interaction with the viral envelope glycoprotein to allow the selective incorporation of the envelope proteins into virus particles. In Rous sarcoma virus, the matrix protein can be chemically cross-linked to the envelope proteins (9), and in HIV-1, the matrix protein has been shown to be required for envelope incorporation (3, 45). Mutations at the 12th and 30th amino acids of the HIV-1 matrix protein blocked envelope incorporation (5), and analysis of revertants incorporating envelope proteins showed that the 34th amino acid may also play a role in envelope incorporation (6). For MuLV, the association between the matrix protein and the envelope protein is still speculative, as there is very little evidence in support of a direct interaction. Truncation of the cytoplasmic tail of the MuLV en-

* Corresponding author. Mailing address: Retrovirus Molecular Biology Group, University of Oxford, Department of Biochemistry, South Parks Rd., Oxford OX1 3QU, United Kingdom. Phone: (1865)275249. Fax: (1865)275259.

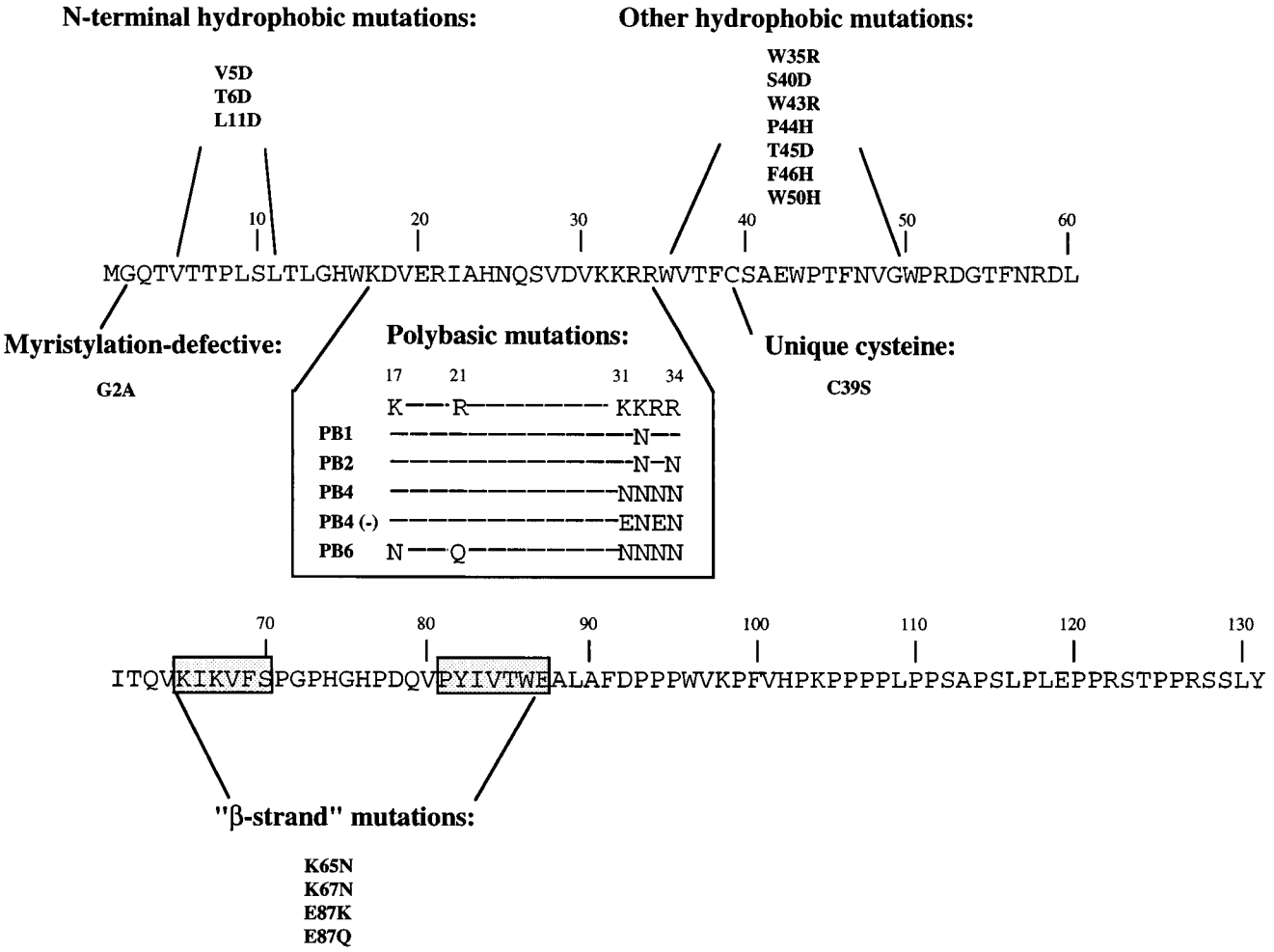

FIG. 1. Amino acid sequence of the Mo-MuLV matrix protein and representation of the mutations made for this study. The Mo-MuLV matrix protein consists of 131 amino acids. Mutations made in various regions of the protein are shown. Boxed sequences show regions predicted to form β-strands by using the secondary structure prediction programs by the methods of Garnier et al. (7), Gascuel and Golmard (8), Novotny and Auffray (26), and Rost and Sander (35, 36).

velope protein (31), and also of that of Rous sarcoma virus (29), does not appear to affect envelope incorporation. This suggests that if an interaction between the matrix protein of MuLV and the envelope glycoprotein does exist, it may occur through the membrane-spanning region of both the envelope protein and the matrix protein or indirectly through another factor.

In this study, we have created two sets of substitution mutations in the Mo-MuLV matrix protein to identify any domains involved in membrane association and envelope incorporation. The first set of mutations was targeted at possible membrane-associating regions, in particular, the polybasic region at the N terminus of the protein, which is similar to the HIV-1 matrix protein, and the regions predicted to form beta strands. The second set of mutations was made within the hydrophobic residues immediately before and after the polybasic region of the MuLV matrix protein to test for the production of virus particles lacking envelope proteins. We have used a replication-defective system (41) to analyze the mutants and have identified regions in the MuLV matrix protein important for cell localization and myristylation. Despite the large number of mutations made, we did not observe any mutant virus particles lacking the envelope glycoproteins, suggesting that a direct interaction between the Mo-MuLV matrix protein and envelope proteins may not exist or that additional factors may be involved.

MATERIALS AND METHODS

Construction of matrix protein mutants. Substitution mutations were made in the matrix protein-coding sequences of the *gag-pol* expression plasmid pHIT60 (41), and these are shown in Fig. 1 and listed in Table 1. Single substitution mutations are designated by the amino acid changed, followed by the position of the amino acid and then the amino acid to which it was changed. Mutations in the polybasic region are designated PB, followed by the number of basic residues changed. PB4 (−) refers to mutations in which four basic residues were altered, some to negatively charged residues, as opposed to all neutral changes in other mutations in this region. Coordinates of the Mo-MuLV genome sequences are as described by Shinnick et al. (39). A 180-bp *Pst*I fragment (coordinates 563 to 743) containing the 5′ sequences of the *gag* gene from p*gag-pol*gpt (21) was excised and inserted into the cloning vector pSP72 (Promega). A 1.2-kb *Bst*EII-*Bgl*II fragment (coordinates 725 to 1906) from p*gag-pol*gpt was subsequently inserted to reconstitute all of the MA and p12 sequences and some of the CA sequences in pSP72. This cloning vector was designated pRV116. Double-stranded synthetic oligonucleotides spanning the *Afl*II site at position 645 and the *Bst*EII site at position 725 and containing mutations within the MA sequence were designed and inserted into pRV116. A 1,090-bp *Afl*II fragment (coordinates 645 to 1735) containing the mutations was then excised from pRV116 and used to replace the corresponding sequences in pRV124, in which the cytomegalovirus (CMV) promoter had been excised from pHIT60 by digestion with *Eco*RI. The CMV promoter was then inserted back into the *Eco*RI site, creating the *gag-pol* expression plasmids encoding mutations in the polybasic region of the matrix

TABLE 1. Virus titers and RT activities of viruses containing mutations in the Mo-MuLV matrix protein[a]

Mutation	Titer (LFU/ml)[b]	RT (% of wt)[c]
Putative membrane-associating regions and cysteine residue		
None	2.6×10^6	100
Basic patch region[d]		
PB1	1.28×10^6	70
PB2	9.6×10^5	56
PB4	3.6×10^5	20
PB4 (−)	4.28×10^2	8.6
PB6	4	6.6
Myristylation defective		
G2A	0	8.0
Other β-strands		
K65N	5.2×10^5	62
K67N	1.6×10^6	128
E87K	1.2×10^6	84
E87Q	9.0×10^5	114
Unique cysteine		
C39S	1.08×10^6	140
Hydrophobic regions		
None	1.5×10^5	100
N terminus		
V5D	3.1×10^3	7.5
T6D	6.8×10^4	30
L11D	9.8×10^4	87
Hydrophobic stretch after basic patch		
W35R	2	2.5
S40D	1.4×10^5	108
W43R	3	3.7
P44H	7.6×10^4	20
T45D	1.7×10^5	135
F46H	1.4×10^5	105
W50H	1	3.7

[a] Both sets of titrations and RT assays were performed three times, and averages were taken for both assays.

[b] LFU, LacZ-forming units (β-galactosidase-positive cells).

[c] The background counts per minute was subtracted from each value, and the relative activities were determined as percentages of wild-type (wt) activities.

[d] Mutations in the basic patch were designated PB, followed by the number of basic residues changed. (−), change of basic residues to acidic residues.

protein. Five matrix protein mutants were created in this manner. In PB1, the 32nd lysine residue was replaced by asparagine. In PB2, the 32nd and 34th residues were changed to asparagine. In PB4, the positively charged lysine and arginine residues found between residues 31 and 34 were all changed to asparagine. In PB4 (−), the 31st and 33rd basic residues have both been changed to glutamic acid, and the 32nd and 34th residues have been changed to asparagine. In PB6, the two basic residues at positions 17 and 21 have been changed to asparagine and glutamine, respectively, in addition to the PB4 mutations described above.

The C39S mutation was created by changing the cysteine codon to a serine codon in a synthetic double-stranded oligonucleotide spanning the *Bst*EII site at coordinate 725 and the *Pst*I site found at position 743. This oligonucleotide was used to replace the corresponding sequences between the *Bst*EII and *Pst*I sites in pRV116. The 1,090-bp *Afl*II fragment containing the mutation was excised and used to replace the corresponding sequences in pRV122, the *gag-pol* expression plasmid containing the PB4 mutation and lacking the CMV promoter. This replacement removes a *Mun*I site created by the mutations in pRV122. The CMV promoter was then inserted back into the *Eco*RI site.

All other mutations were introduced by oligonucleotide-directed mutagenesis. A 1,220-bp *Eco*RI-*Xho*I fragment (coordinates 340 to 1560) (the *Eco*RI site is the result of a deletion in the packaging signal) (21) containing all of the MA sequences and extending into the CA sequences was isolated from pHIT60 and inserted into the *Eco*RI-*Sal*I sites in pAlter-1 (Promega). Oligonucleotides were designed, and site-directed mutagenesis was performed by using the Altered Sites Mutagenesis System (Promega) according to the manufacturer's recommendations. First, the G2A mutation was introduced into pHIT60. A 305-bp *Eco*RI-*Afl*II fragment (coordinates 340 to 645) containing the mutation was isolated from pAlter-1 and replaced the corresponding sequences in pHIT60 which lacked the CMV promoter. The CMV promoter was inserted back into this plasmid at the *Eco*RI site. To introduce the K65N and K67N mutations independently into pHIT60, a 160-bp *Bst*EII-*Sty*I fragment (coordinates 725 to 885) containing the mutation replaced the corresponding sequences in pRV116. The 1,090-bp *Afl*II fragment was then excised and used to replace the 1,090-bp *Afl*II sequences in pRV122. The CMV promoter was finally inserted into the *Eco*RI site. For the E87K and E87Q mutations, 535-bp *Bst*EII-*Bsm*I fragments (coordinates 725 to 1260) containing the mutations were isolated from pAlter-1 and replaced the corresponding sequences in pRV116. The 1,090-bp *Afl*II fragment was then excised and used to replace the 1,090-bp *Afl*II sequences in pRV122. The CMV promoter was replaced by insertion into the *Eco*RI site.

All mutations introduced in the hydrophobic residues were similarly created by oligonucleotide-directed mutagenesis of pAlter-1 containing the *Eco*RI-*Xho*I fragment from p*gag-pol*gpt (21) as described above. First, the *gag-pol* expression plasmid containing the S40D mutation was created to simplify subsequent cloning steps for the remaining constructs. A 535-bp *Bst*EII-*Bsm*I fragment (coordinates 725 to 1260) containing the S40D mutation was excised and inserted into a pSP72 vector (Promega) containing the same *Eco*RI-*Xho*I *gag* fragment as described above. The S40D mutation destroys the *Pst*I site at position 743. The *Eco*RI-*Xho*I fragment containing the mutation was then excised and replaced the corresponding sequences of the *gag-pol* expression plasmid containing the PB4 mutation, destroying a *Mun*I site and creating a *gag-pol* expression plasmid containing the S40D mutation. To introduce the V5D and T6D mutations, the 920-bp *Eco*RI-*Bsm*I fragments (coordinates 340 to 1260) containing the mutations were excised from pAlter-1 and replaced the corresponding *gag* sequences containing the S40D mutation in pSP72 (see above), restoring the *Pst*I site. All subsequent steps were the same as for the S40D mutation. The L11D and W35R mutations were created by isolating a 615-bp *Afl*II-*Bsm*I fragment (coordinates 645 to 1260) containing the mutations, and the W43R, P44H, T45D, F46H, and W50H mutations were all created by replacing a 540-bp *Bst*EII-*Bsm*I fragment from the pAlter-1 vector and placing it into the pSP72 vector containing the S40D mutation to restore the *Pst*I site. All fragments isolated from pAlter-1 following mutagenesis were completely sequenced.

Cell lines, transfections, and infections. 293T cells (4), NIH 3T3 cells, and COS-1 cells were maintained in Dulbecco's modified Eagle medium supplemented with 10% fetal calf serum, 1 mM glutamine, and antibiotics. Three-plasmid cotransfections and virus titrations were performed as previously described (41).

Western blot analysis of cellular extracts and virus particles. 293T cells were transfected, and viral supernatants and cells were harvested 48 h posttransfection. Viral supernatants were filtered through a 0.45-μm-pore-size filter, and 1.5 ml of the supernatant was spun in a microcentrifuge for 30 min at 4°C. Virus pellets were washed with phosphate-buffered saline and resuspended in sodium dodecyl sulfate-polyacrylamide gel electrophoresis (SDS-PAGE) loading buffer. Cells were lysed in protein lysis buffer (9 M urea, 50 mM Tris [pH 7.4], 1% β-mercaptoethanol) and centrifuged. Protein concentrations were determined by the Bradford protein assay. The proteins were analyzed by SDS–12.5% PAGE and immunoblotted with either the monoclonal anti-p12 F548 antibody (ATCC CRL 1890) or an anti-p15 (MA) antibody raised in rabbit for the detection of *gag* proteins or with the anti-Rauscher leukemia virus (anti-RLV) gp69/71 *env* antibody (Quality Biotech, Inc.) for the detection of *env* proteins. Proteins were visualized by enhanced chemiluminescence (Amersham).

RT assays. Reverse transcriptase (RT) assays were performed as previously described (10). Briefly, 90 μl of filtered viral supernatants was added to 10 μl of 10× reaction cocktail [500 mM Tris-HCl (pH 8.3), 0.5% Nonidet P-40 (NP-40), 50 μg of oligo(dT) per ml, 100 μg of polyriboadenylic acid per ml], and 10 μCi of [α-^{32}P]dTTP (specific activity, 3,000 Ci/mmol; Amersham) was added per 100 μl of the reaction mixture. The reaction mixture was incubated at 37°C for 2 h, and 5 μl of each reaction mix was spotted directly onto dry DEAE-paper (DE-81; Whatman, Inc.). The paper was washed three times for 15 min each with gentle rocking at room temperature in 0.6 M NaCl–0.06 M sodium citrate and then twice with 95% ethanol. The paper was dried, and radioactivity was counted in a scintillation counter.

Metabolic labelling of cells and radioimmunoprecipitation analyses of viral proteins. Cells were labelled with 500 μCi of [^{3}H]myristic acid (NEN Research Products) per ml for 20 h in Dulbecco's modified Eagle medium supplemented with 10% fetal calf serum, 1 mM sodium pyruvate, 1 mM nonessential amino acids, 1 mM glutamine, 1% penicillin-streptomycin, and 1% dimethyl sulfoxide. After the labelling, cells were washed with phosphate-buffered saline and then lysed in radioimmunoprecipitation assay (RIPA) buffer (0.12 M NaCl, 20 mM Tris [pH 8.0], 1% NP-40, 0.2% sodium deoxycholate, 0.2% SDS) with proteinase inhibitors (100 μg of phenylmethylsulfonyl fluoride per ml, 50 U of aprotinin per ml, 1 μg of pepstatin A per ml, and 1 μg of leupepsin per ml). The cells were centrifuged in a microcentrifuge for 10 min at 4°C, and the supernatants were precleared first with mouse serum on agarose, then with protein A on agarose, and finally with protein G-Sepharose (Pharmacia). The samples were treated with a monoclonal anti-p12 F548 antibody (ATCC CRLL 1890) for 2 h at 4°C and subsequently with 50 μl of protein G-Sepharose for 1 1/2 h at 4°C. The protein G-Sepharose beads were washed twice with RIPA buffer, once with

high-salt buffer (2 M NaCl, 10 mM Tris [pH 7.4], 1% NP-40, 0.5% sodium deoxycholate), and once again with RIPA buffer. SDS-PAGE loading buffer was added to the washed beads and boiled for 5 min, and the immunoprecipitates were removed from the beads by centrifugation. The proteins were separated on an SDS–12.5% polyacrylamide gel, and the gel was fixed in 50% methanol–10% acetic acid, treated with Amplify (Amersham), and exposed to preflashed X-ray film (Hyperfilm-MP; Amersham).

Localization of viral proteins by indirect immunofluorescence. Cells were grown on coverslips and transfected. At 48 h after transfection, the cells were fixed in 3% paraformaldehyde for 30 min at room temperature. The cells were then washed for 5 min with 10 mM glycine and permeabilized with 1% Triton X-100 for 5 min. Subsequent washes consisted of 5 min with 10 mM glycine, 30 min with 25 mM glycine, and 5 min with 10 mM glycine. The cells were blocked with 3% normal mouse serum–1% bovine serum albumin–0.5 M NaCl–0.05% Tween 20 for 5 h at room temperature. The monoclonal anti-p12 F548 antibody (ATCC CRL 1890) was then added undiluted and left overnight at 4°C. Before addition of the secondary antibody, the cells were washed twice with 10 mM glycine for 10 min. A 1:100 dilution of fluorescein-conjugated sheep anti-mouse immunoglobulin (Amersham) was added to the cells in the same solution as in the blocking step and left for 2 1/2 h at room temperature in the dark. The cells were washed again twice in 10 mM glycine for 10 min, and the coverslips were mounted onto slides. Cells were observed with a 100× oil immersion objective on a Zeiss Axiovert microscope. At least 20 fields were observed, totalling approximately 50 transfected cells, and cells representative of the transfected population were photographed.

Electron microscopy. 293T cells were transfected with the wild-type *gag-pol* expression construct pHIT60 or the mutant constructs. Cells were harvested and fixed in 2.5% glutaraldehyde–300 mM sodium cacodylate buffer (pH 7.4) at 48 h posttransfection. The cells were maintained in the fixing solution at 4°C until further manipulation. Cells were prepared and examined by electron microscopy as previously described (15).

RESULTS

Effect of mutations in the polybasic region and putative β-strands of Mo-MuLV MA. We have previously described a convenient system for producing high-titer retroviral vectors (HIT vectors) useful for gene transfer applications and for analyzing a large number of *gag-pol* or *env* mutants (41). We have used this system in this study to identify functional domains of the Mo-MuLV matrix protein responsible for cell localization and incorporation of the viral envelope glycoproteins into virus particles. Two sets of mutations were made in the matrix protein-coding sequence of the *gag-pol* expression plasmid, pHIT60 (41), creating a total of 21 mutants (Fig. 1). The first series of mutations made were based upon data reported for the HIV-1 matrix protein, placing emphasis on the polybasic region found in the first 34 amino acids of the Mo-MuLV matrix protein and on regions predicted to form β-strands (Fig. 1). Secondary-structure prediction analysis was performed by using four different programs, which included the methods of Garnier et al. (7), Gascuel and Golmard (8), Novotny and Auffray (26), and Rost and Sander (35, 36). The results from the four programs were compared. Two regions in the Mo-MuLV matrix protein were predicted to form β-strands in all four analyses (Fig. 1). In the first region (residues 65 to 70), we changed two positively charged residues, and in the other region, (residues 81 to 87), we altered a negatively charged glutamic acid. The second set of mutations was created in an attempt to search for residues involved in the interaction with the envelope glycoproteins, focusing on hydrophobic residues surrounding the polybasic region on the basis of some speculation that a membrane-penetrating region of the matrix protein may be involved. Viruses carrying mutations within the matrix protein were first assessed for their ability to infect NIH 3T3 cells. 293T cells were cotransfected with a *gag-pol* expression plasmid, pHIT123 (the ecotropic envelope expression plasmid), and pHIT111 (the proviral vector plasmid carrying the neomycin resistance and *lacZ* genes). Viral supernatants were harvested and used to transduce NIH 3T3 cells, which were assayed for β-galactosidase activity as previously described (41).

Three mutations from the first set, PB6, PB4 (−), and G2A, caused a substantial reduction in virus titer and RT activity (Table 1). Other mutations in the polybasic region, PB1, PB2, and PB4, caused a slight reduction in both virus titer and RT activity, as did the K65N mutation in the first putative β-strand (Table 1). Western blot analysis was next performed to test for the production of virus particles. Immunoblotting of cell extracts with an anti-p12 monoclonal antibody showed that all of the mutants are capable of producing *gag* proteins at almost wild-type levels (Fig. 2A). The *env* protein was also produced at the same levels as for the wild type by all of these mutants (Fig. 2B). As expected, no virus particles were detected in viral supernatants from cells expressing the PB6, PB4 (−), and G2A mutants (Fig. 2C and D, lanes 3, 4, and 7, respectively). Mutations PB1, PB2, PB4, and K65N, which caused more subtle reductions in virus titer (Table 1), showed detectable amounts of virus particles in the supernatant, albeit at levels lower than wild type (Fig. 2C, lanes 1, 2, 6, 8, and 9). Envelope incorporation was not affected by these mutations, as the ratio between the amounts of *gag* and *env* proteins in the viral supernatants did not appear to be different from that for the wild type (Fig. 2C and D, lanes 1, 2, 6, 8, and 9). The lack of virus production resulting from the G2A mutation, which should impair myristylation of the matrix protein, was expected (38).

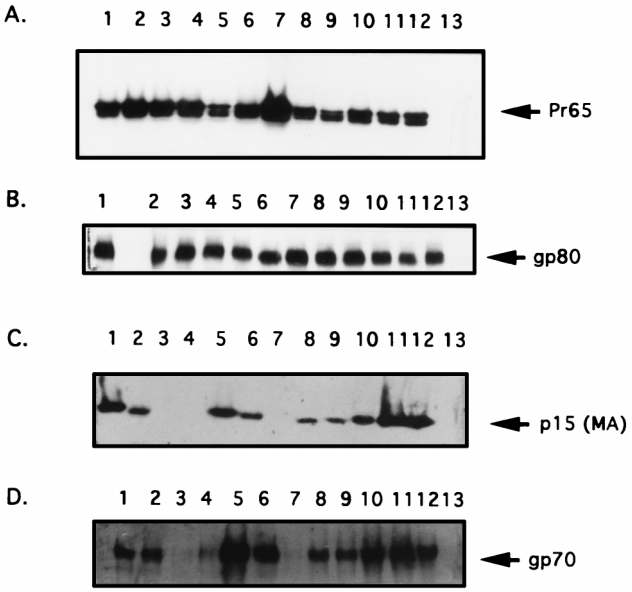

FIG. 2. Western blot analysis of viral proteins and virus particles with mutations in the putative membrane-associating region and the cysteine residue of the matrix protein. 293T cells were transfected with pHIT123, pHIT111, and pHIT60 (lanes 1) or the *gag-pol* expression plasmids containing the MA mutation PB4 (lanes 2), PB6 (lanes 3), PB4 (−) (lanes 4), C39S (lanes 5), PB1 (lanes 6), G2A (lanes 7), PB2 (lanes 8), K65N (lanes 9), E87K (lanes 10), K67N (lanes 11), or E87Q (lanes 12). Untransfected cells served as a negative control (lanes 13). Cell extracts were immunoblotted with an anti-p12 *gag* F548 monoclonal antibody (A) and an anti-RLV gp69/71 *env* antibody (B). Viral supernatants were harvested, pelleted, and immunoblotted with an anti-p15 *gag* antibody raised in rabbit (C) and an anti-RLV gp69/71 *env* antibody (D).

Myristylation of *gag* proteins with mutations in the polybasic region of MA. Myristylation has been shown to play an important role in the assembly of MuLV (33), and as stated above, the lack of virus production resulting from the G2A mutation is probably due to a defect in myristylation, since this amino acid change has been previously shown to prevent myristylation of the matrix protein (38). It was our assumption that the matrix proteins harboring the PB4 (−) and PB6 mutations were properly myristylated, but this assumption was tested.

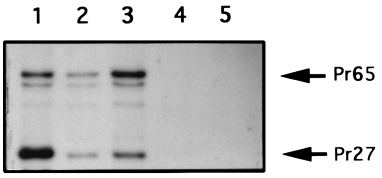

FIG. 3. Myristylated MuLV-specific *gag* proteins from cells expressing the basic patch mutants of MA. 293T cells were transfected with pHIT60 (lane 1) or the *gag-pol* expression plasmid containing the MA mutation PB6 (lane 2) or PB4 (−) (lane 3). Cells transfected with the *gag-pol* expression plasmid containing the MA mutation G2A (lane 4) and untransfected cells (lane 5) served as negative controls. Cells were labelled with 500 μCi of [^{3}H]myristic acid (NEN Research Products) per ml for 20 h. Cell lysates were immunoprecipitated with a monoclonal anti-p12 *gag* F548 antibody, and the same amount of protein from each sample was loaded onto an SDS–12.5% polyacrylamide gel. The dried gel was exposed to presensitized film.

293T cells were transfected with the mutant constructs and labelled with [^{3}H]myristic acid, followed by immunoprecipitation with an anti-p12^{gag} monoclonal antibody. The G2A mutant served as a negative control. As Fig. 3 shows, compared with the wild type (lane 1), *gag* proteins containing the PB6 mutation were incompletely myristylated (lane 2), while the precursor form, Pr65^{gag}, containing the PB4 (−) mutation in the matrix protein, was completely myristylated (lane 3). As expected, the G2A mutation prevented the production of myristylated products (Fig. 3, lane 4).

Analysis of particle formation by electron microscopy. 293T cells expressing wild-type or mutant PB4 (−) *gag* proteins were next analyzed for particle formation by electron microscopy, since the PB6 mutant showed a defect in myristylation. Cells transfected with the wild-type *gag-pol* construct, pHIT60, showed only extracellular budding (Fig. 4A) and no intracellular assembly of virus particles (data not shown). Small, dense patches of protein could be detected accumulating at the endoplasmic reticulum in cells transfected with the *gag-pol* construct containing the MA PB4 (−) mutation (Fig. 4B and C). Formation of more-complete spherical structures not associated with cell membranes could also be detected in the cytoplasm of these cells (Fig. 4D); all virus-like particles were intracellular, and no extracellular budding was observed (data not shown). In contrast, no protein accumulation or formation of virus particles was detected in cells expressing the myristylation-defective *gag* protein (data not shown). Taken together, these data provide evidence for the importance of N-terminal basic residues of the MuLV matrix protein in directing particle assembly and cellular localization of *gag* proteins.

Virus titers are reduced with changes at the N-terminal hydrophobic residues and tryptophan residues at positions 35, 43, and 50. A total of 10 mutations were introduced in the N-terminal hydrophobic residues preceding the basic patch and the hydrophobic region found immediately after the cluster of basic residues (Fig. 1). Mutations at tryptophan residues 35, 43, and 50 resulted in the generation of virus stocks with no infectivity or significant RT activity (Table 1), while other mutations resulted in the generation of virus stocks with relatively high titers, with the exception of V5D, T6D, and P44H, which appeared to cause some reduction in virus titer and RT activity (Table 1). Low virus production and infectivity could not be due to the lack of *gag* and *env* protein synthesis, as both proteins were produced at almost wild-type levels by all of the mutants (Fig. 5A and B). However, both *gag* and *env* proteins were undetectable in supernatants of cells expressing all three tryptophan mutants (Fig. 5C and D, lanes 5, 7, and 11) or were detected at slightly lower levels in the supernatant of the MA mutant P44H (Fig. 5C and D, lanes 8). Low levels of particles were also detected in the supernatant of the MA mutant V5D (Fig. 5C and D, lanes 2), while the MA T6D mutant contained more virus particles in the supernatant than the V5D mutant (Fig. 5C and D, lanes 2 and 3). This suggests that these mutations may have affected particle release, and therefore, this aspect was investigated next.

Incomplete myristylation by mutation of N-terminal hydrophobic residues. Since N-terminal residues can affect myristylation, myristylation of *gag* proteins containing the MA mutations V5D and T6D was examined. Although mutations further downstream of the myristylation site should not affect proper myristylation, other mutants with the most profound effect on virus titer and particle release were also examined, which included mutants with changes at tryptophan residues located at positions 35, 43, and 50. The mutation V5D clearly caused a defect in myristylation of the *gag* protein, while the mutation T6D still allowed myristylation of the *gag* protein but at a slightly lower efficiency than for the wild type (Fig. 6A). The same two residues were changed to similar hydrophobic residues in a previous study, but both mutations did not appear to affect proper myristylation of the *gag* proteins (12). In our study, the two hydrophobic residues were mutated to charged residues, which may have disrupted the hydrophobicity of the N terminus of the matrix protein, causing an impairment in myristylation.

The tryptophan mutations W35R, W43R, and W50H did not affect proper myristylation of Pr65^{gag}, although the Pr27 cleavage product was detected at much lower levels than with the wild type (Fig. 6B). This suggests that at least part of the defect in these three mutants may be incomplete cleavage of the *gag* precursor. However, this should not affect the budding of particles from the cell.

Indirect immunofluorescence shows perinuclear localization of tryptophan mutants. Although cleavage of the *gag* precursor is not necessary for release of virus particles from the cell, we speculated that the lack of cleavage products from the W35R, W43R, and W50H mutants may be due to a block in transport of the *gag* precursors to the cell membrane, despite proper myristylation. Since the defect in mutants carrying changes at the N terminus of MA was shown to be a result of incomplete myristylation, the cause of the defects in the tryptophan mutants was examined. Indirect immunofluorescence analysis was performed on cells expressing the tryptophan mutants to determine the localization of the *gag* proteins. Cells expressing the tryptophan mutants all showed similar staining patterns, but these were distinctly different from that of cells expressing the wild-type protein (Fig. 7). Cells expressing the wild-type *gag* protein showed some punctate staining at the cell periphery and inside the cells as well as some staining near the nucleus (Fig. 7A). In contrast, all three tryptophan mutants appeared to produce *gag* proteins which localized mostly around the nucleus in a diffuse manner with no punctate staining (Fig. 7B, C, and D). Despite normal myristylation of the *gag* precursor, Pr65^{gag} (Fig. 6B), it is clear that the mutant *gag* proteins are not being transported to the inner leaflet of the plasma membrane. Retention of *gag* proteins in the cytoplasm may also explain the absence of cleavage products from the tryptophan mutants in Fig. 6B, as proteolytic cleavage occurs during budding from the membrane. Assembly of virus particles was not detected in cells expressing these mutants when observed by electron microscopy (data not shown).

DISCUSSION

We approached the functional analysis of the Mo-MuLV matrix protein by a mutagenesis study in which regions of the MuLV matrix protein similar to those of the HIV-1 matrix

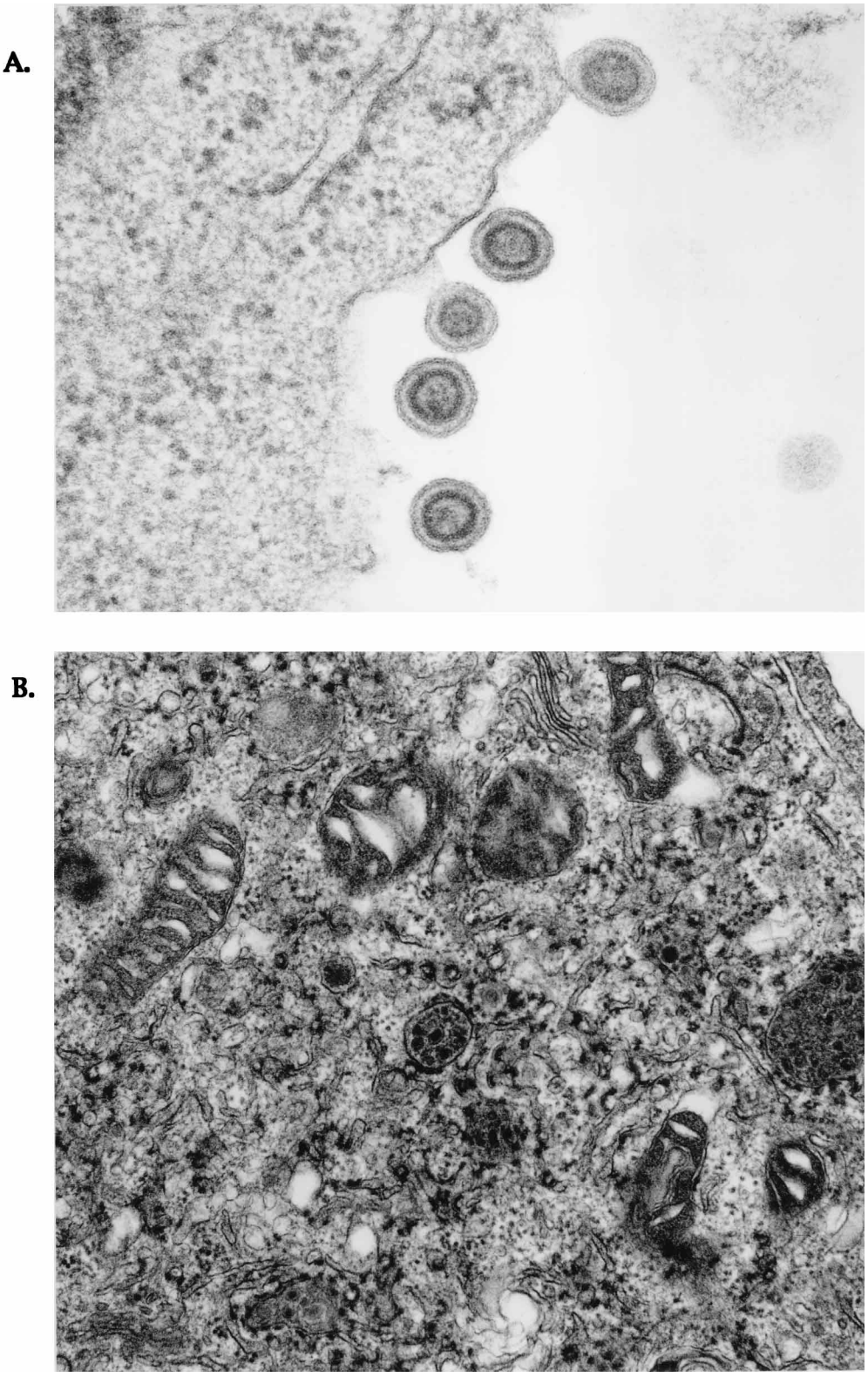

FIG. 4. Electron microscopy of cells expressing the MA basic patch mutant PB4 (−). Cells were harvested and fixed at 48 h posttransfection in 2.5% glutaraldehyde–300 mM sodium cacodylate buffer (pH 7.4). Sections were prepared and cut as previously described (15) and examined with a Philips CM12 microscope. (A) Extracellular budding of wild-type (pHIT60) particles. Magnification, ×108,000. (B) Intracellular accumulation of proteins in cells expressing the PB4 (−) mutant. Magnification, ×41,000. (C) Accumulation of proteins at the endoplasmic reticulum in cells expressing the PB4 (−) mutant. Magnification, ×84,000. (D) Formation of intracellular virus-like particles in cells expressing the PB4 (−) mutant. Magnification, ×84,000.

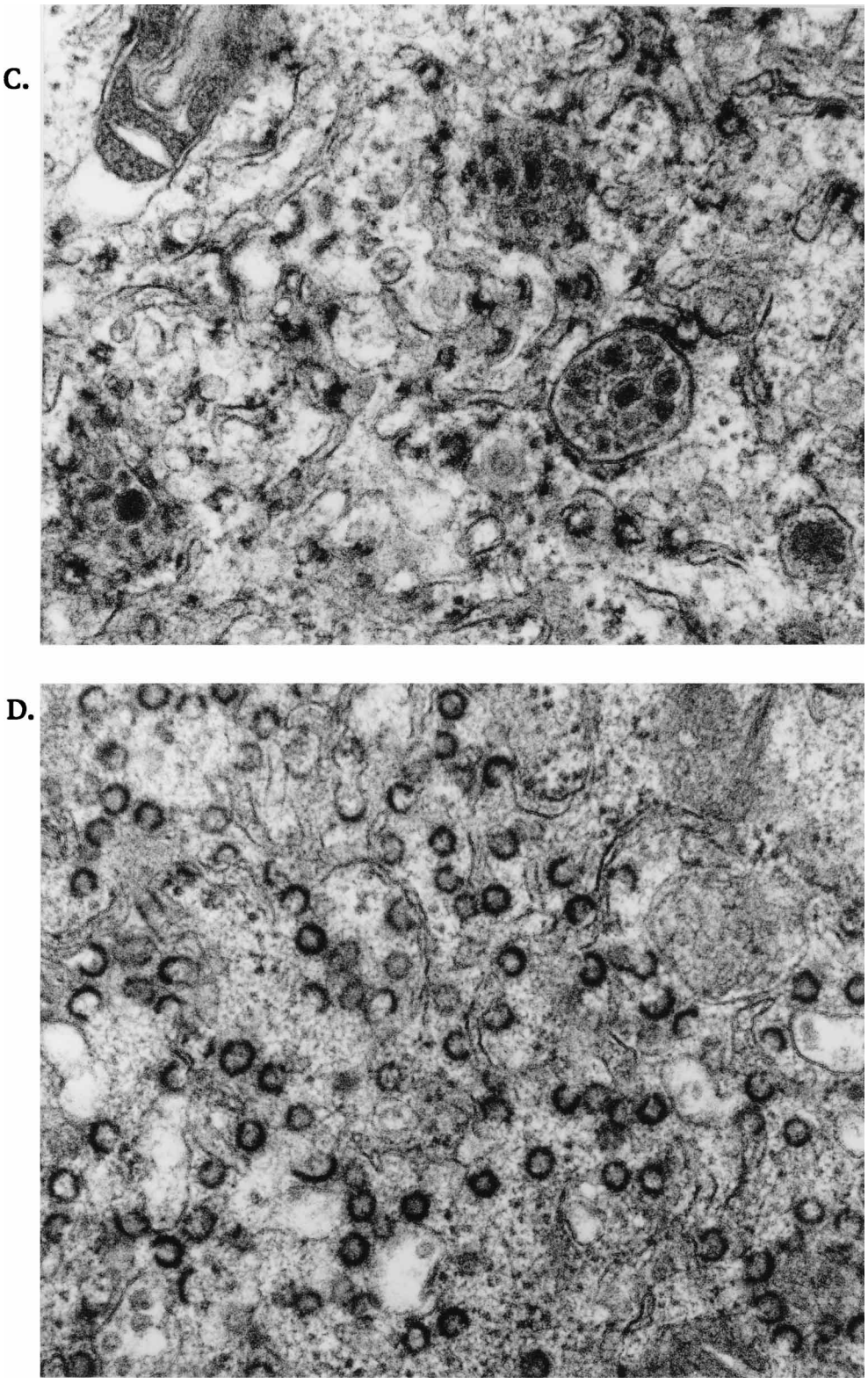

FIG. 4—*Continued.*

protein were chosen to test for functional analogies. In particular, regions which may be involved in interaction with the phospholipid head groups of the plasma membrane or the viral envelope glycoproteins were examined. We have constructed 21 matrix protein mutants to address these two issues and have analyzed them by using a replication-defective retroviral system that we have developed previously (41).

In the first instance, we sought to determine the significance

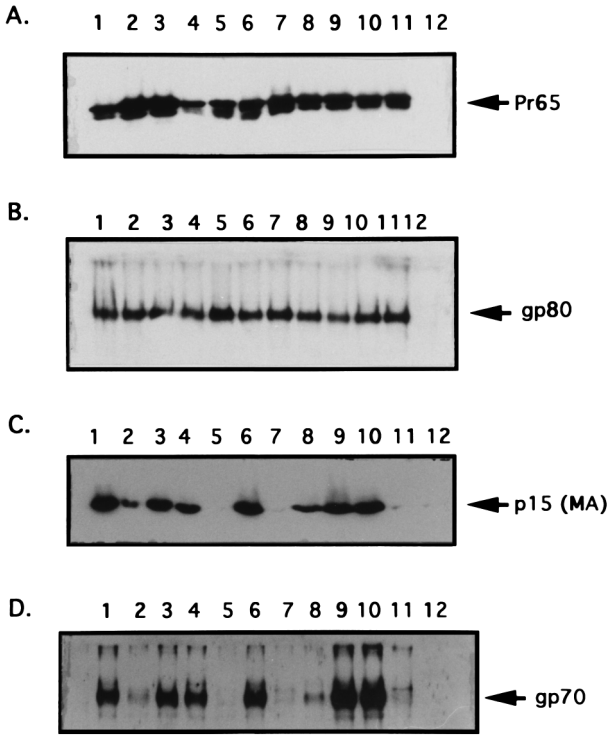

FIG. 5. Western blot analysis of mutant proteins and virus particles of the hydrophobic matrix mutants. 293T cells were transfected with pHIT123, pHIT111, and pHIT60 (lanes 1) or the *gag-pol* expression plasmid containing the MA mutation V5D (lanes 2), T6D (lanes 3), L11D (lanes 4), W35R (lanes 5), S40D (lanes 6), W43R (lanes 7), P44H (lanes 8), T45D (lanes 9), F46H (lanes 10), or W50H (lanes 11). Untransfected cells served as a negative control (lanes 12). Cell extracts were immunoblotted with an anti-p12 *gag* F548 monoclonal antibody (A) and an anti-RLV gp69/71 *env* antibody (B). Viral supernatants were harvested, pelleted, and immunoblotted with an anti-p15 *gag* antibody raised in rabbit (C) and an anti-RLV gp69/71 *env* antibody (D).

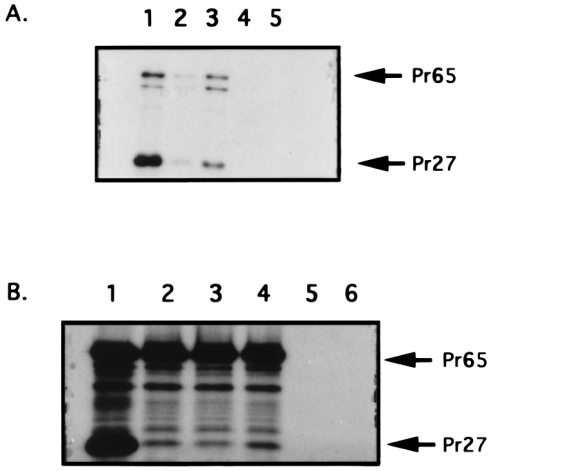

FIG. 6. Myristylated MuLV-specific *gag* proteins from cells expressing N-terminal and tryptophan mutants. 293T cells were transfected and labelled with 500 μCi of [^{3}H]myristic acid (NEN Research Products) per ml for 20 h. Cell lysates were immunoprecipitated with a monoclonal anti-p12 *gag* F548 antibody, and the same amount of protein from each sample was loaded onto an SDS–12.5% polyacrylamide gel. The dried gel was exposed to presensitized film. (A) Myristylated *gag* products from cells transfected with pHIT60 (lane 1) or the *gag-pol* expression plasmid containing the V5D mutation (lane 2) or the T6D mutation (lane 3). Cells expressing the G2A mutant (lane 4) and untransfected cells (lane 5) served as negative controls. (B) Myristylated *gag* products from cells transfected with pHIT60 (lane 1) or the *gag-pol* expression plasmid containing the W35R mutation (lane 2), the W43R mutation (lane 3), or the W50H mutation (lane 4). Cells expressing the G2A mutant (lane 5) and untransfected cells (lane 6) again served as negative controls.

of six positively charged residues clustered at the N terminus of the Mo-MuLV matrix protein. In analyzing the role of the cluster of basic residues, we made incremental changes to this region. Interestingly, substitution of one basic residue had little effect on virus production (Table 1, PB1). A recent report also suggested that single changes to the basic residues of the Mo-MuLV matrix protein do not affect normal function of the protein (12). However, with each additional change of a positively charged residue to a neutral residue, we observed that the virus titer decreased (Table 1, PB1, PB2, PB4, and PB6). A very similar effect was seen with the HIV-1 matrix protein when deletions or substitution mutations were made in the N-terminal polybasic region (46). When only three basic residues were replaced by acidic residues, no significant change in virus phenotype was observed. When the substitutions or deletions affected more than three basic residues, virus production was abolished and proteins accumulated in the cytoplasm. The gradual decrease in virus titer with increased substitutions suggests that the extent of membrane association may be proportional to the net positive charge in the basic patch region, as has been shown for several proteins, including the Ras protein (13) and the Src protein (40). In fact, the most significant effect on Mo-MuLV production was seen when the net charge between residues 31 and 34 of MA was changed to negative [Table 1, PB4 (−)]. It is known that phosphorylation of proteins, such as the MARCKS protein (20), can cause electrostatic repulsion from the acidic phospholipids of the plasma membrane by decreasing the membrane-binding energy and can cause the protein to become released from the plasma membrane. The incorporation of acidic amino acids in the polybasic region of the Mo-MuLV matrix protein most likely had the same effect. Also for this MA basic patch mutant, PB4 (−), immunofluorescence analysis showed that the mutant *gag* protein did not localize at the plasma membrane but localized in the cytoplasm in a punctate manner (data not shown), despite proper myristylation (Fig. 3). Previous studies have suggested that MuLV *gag* proteins travel to the plasma membrane via vesicular transport by association with the cytoplasmic face of intracellular vesicles (14, 17). It was therefore possible that the punctate staining pattern observed in cells expressing the PB4 (−) mutant (data not shown) was due to mutant *gag* proteins localizing at intracellular membranes. Subcellular fractionation results supported this speculation, as much of the mutant *gag* proteins was isolated in the membrane fraction (data not shown) and analysis of cells by electron microscopy techniques showed large amounts of dense protein accumulating at the endoplasmic reticulum when cells were transfected with the mutant construct (Fig. 4B and C). Assembly into virus-like particles was also detected in the cytoplasm (Fig. 4D), but no extracellular budding could be seen, suggesting that the mutant particles were impaired in transport to the membrane as a result of the mutations made in the N-terminal basic residues.

The structure of the HIV-1 matrix protein (22, 23) showed that the basic residues lie in a β-sheet, and therefore, mutations were also introduced in the Mo-MuLV MA where β-strands were predicted to form (Fig. 1). Mutations in the predicted regions had no significant effect, except for the lysine residue at position 65, which caused a slightly reduced virus titer and RT activity compared to the wild type (Table 1). This additional charge may be brought into close proximity to the

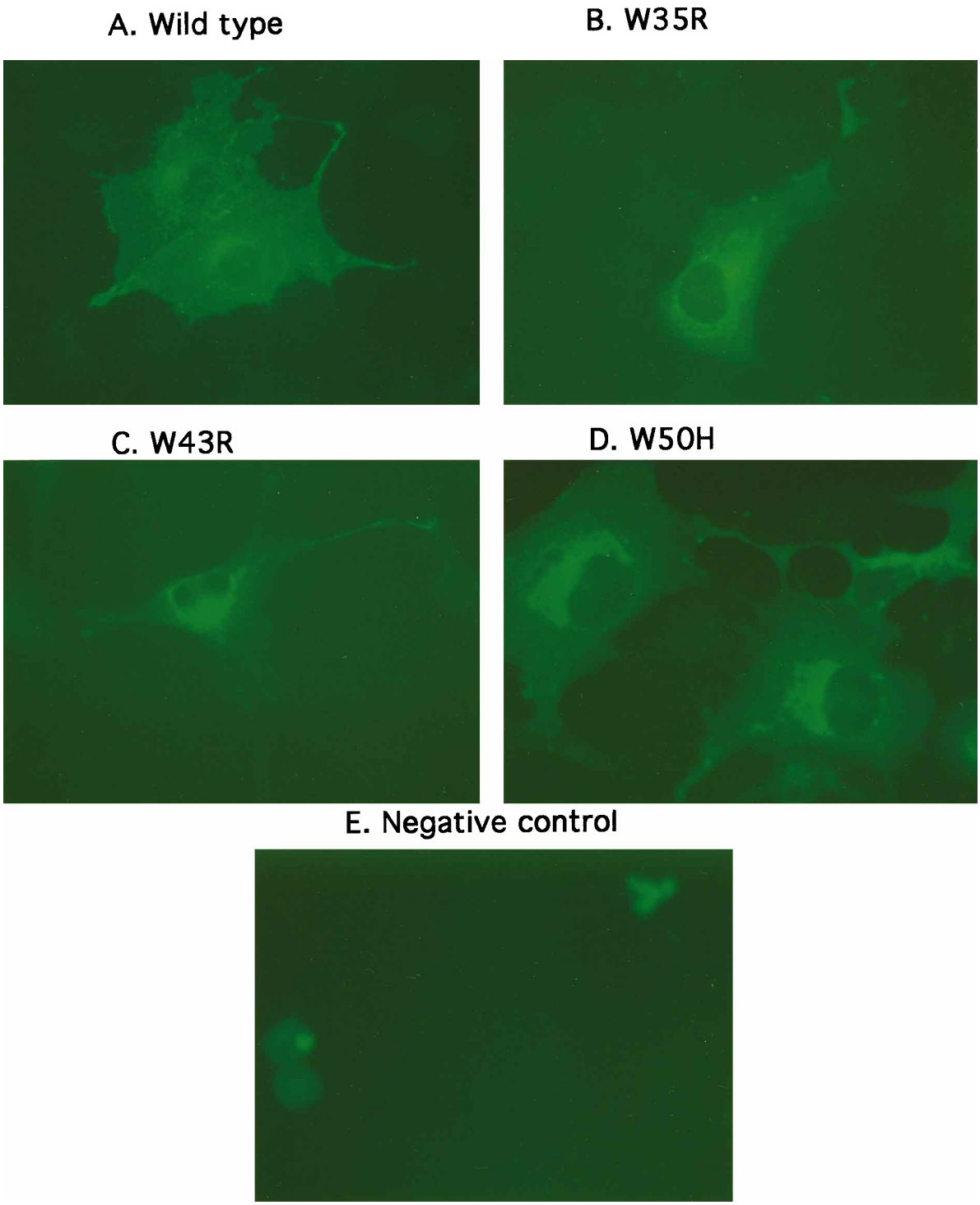

FIG. 7. Intracellular distribution of the tryptophan mutants determined by indirect immunofluorescence. Cells transfected with pHIT60 (A) or the *gag-pol* expression plasmid containing the W35R mutation (B), the W43R mutation (C), the W50H mutation (D), or untransfected cells (E) were fixed in 3% paraformaldehyde and permeabilized with 1% Triton X-100 at 48 h posttransfection. The primary antibody was a monoclonal anti-p12 *gag* F548 antibody, and the secondary antibody was a fluorescein-conjugated anti-mouse immunoglobulin. Cells were observed under a 100× oil immersion objective with a Zeiss Axiovert microscope.

plasma membrane by the folding of the region into a β-sheet, to contribute to the electrostatic attraction between the matrix protein and the phospholipids of the membrane. Clearly, confirmation of this notion awaits structural analysis of the matrix protein.

We next focused on identifying regions of interaction between the matrix protein and the envelope glycoproteins, and we chose hydrophobic stretches immediately before and after the polybasic region, mainly because we speculated that if a direct interaction exists, it would occur between the membrane-spanning domain of the envelope protein and a mem-

brane-penetrating region of the matrix protein. Our assumptions were based on reports that the cytoplasmic tail of the envelope protein is dispensable for envelope incorporation (29, 31). Mutations of the chosen hydrophobic residues failed to produce virus particles with a reduction in envelope incorporation. This was not surprising, however, because a previous study reported that replacement of the transmembrane domain of the MuLV envelope protein with a glycosylphosphatidylinositol membrane anchor did not affect envelope incorporation into virions (30), suggesting that all or part of the membrane-spanning region and the cytoplasmic tail may be dispensable for envelope incorporation. More recently, swapping of the transmembrane domains of the MuLV and human T-cell leukemia virus type 1 envelope proteins demonstrated that all of the membrane-anchoring domain and the cytoplasmic tail of MuLV may not be required for envelope incorporation (2). We were also unable to find any mutations in the hydrophobic region of the matrix protein that reduced envelope incorporation, further supporting the notion that a specific single interaction may not exist.

During our search for envelope-interacting regions, we have discovered that the fifth and sixth amino acids of the Mo-MuLV matrix protein are important for proper myristylation (Fig. 6A), and this is in agreement with the requirements for myristylation of the closely related Akv MuLV matrix protein (18). Surprisingly, the PB6 mutation, which affected six basic residues, with the first mutation occurring at position 17 (Fig. 1), prevented complete myristylation of the *gag* proteins (Fig. 3, lane 2). Short stretches of amino acids following the myristylation site have been known to influence myristylation (19, 28), but involvement of residues further downstream was not expected. Mutations affecting 20 amino acids downstream from the N terminus of the HIV-1 matrix protein also appeared to cause a reduction in myristylation (46). It is possible that these mutations affected the three-dimensional structures of the proteins and prevented the exposure of the N-terminal region for myristylation.

We have also found that mutation of tryptophan residues completely abrogated virus production (Table 1). All three tryptophan mutants clearly showed a cellular localization different from that of the wild type (Fig. 7), suggesting that tryptophan residues may play an important role in intracellular transport of *gag* proteins. However, it is also possible that improper folding of the mutant *gag* proteins could obscure the myristyl group or the N-terminal basic patch, rendering the two regions unavailable for interaction with the plasma membrane.

All retroviral matrix proteins appear to play similar roles in the retrovirus life cycle, particularly in virus assembly. Despite the lack of sequence homology between the lentiviral and type C retroviral matrix proteins, they seem to possess functionally homologous regions, as evidenced by mutagenesis analysis of the polybasic region. However, there are clearly differences, as demonstrated by our inability to use the HIV model to identify residues involved in envelope retention. Further understanding of the functions of the matrix protein would be greatly enhanced by structural information, and towards this end, we have recently produced crystals of the protein. It remains to be seen whether the matrix proteins of all retroviruses are structurally similar.

ACKNOWLEDGMENTS

We thank David Hockley at the National Institute for Biological Standards and Control (NIBSC) for performing electron microscopy.

Y.S. is a recipient of the Overseas Research Scheme (ORS) Award and the Oxford Kobe Scholarship.

REFERENCES

1. **Bigay, J., E. Faurobert, M. Franco, and M. Chabre.** 1994. Roles of lipid modifications of transducin subunits in their GDP-dependent association and membrane binding. Biochemistry **33:**14081–14090.
2. **Denesvre, C., C. Carrington, A. Corbin, Y. Takeuchi, F.-L. Cosset, T. Schulz, M. Sitbon, and P. Sonigo.** 1996. TM domain swapping of murine leukemia virus and human T-cell leukemia virus envelopes confers different infectious abilities despite similar incorporation into virions. J. Virol. **70:**4380–4386.
3. **Dorfman, T., F. Mammano, W. A. Haseltine, and H. G. Göttlinger.** 1994. Role of the matrix protein in the virion association of the human immunodeficiency virus type 1 envelope glycoprotein. J. Virol. **68:**1689–1696.
4. **Dubridge, B. B., H. C. Hsia, P.-M. Leong, J. H. Miller, and M. P. Carlos.** 1987. Analysis of mutation in human cells by using an Epstein-Barr virus shuttle system. Mol. Cell. Biol. **7:**379–387.
5. **Freed, E. O., and M. A. Martin.** 1995. Virion incorporation of envelope glycoprotein with long but not short cytoplasmic tails is blocked by specific, single amino acid substitutions in the human immunodeficiency type 1 matrix. J. Virol. **69:**1984–1989.
6. **Freed, E. O., and M. A. Martin.** 1996. Domains of the human immunodeficiency virus type 1 matrix and gp41 cytoplasmic tail required for envelope incorporation into virions. J. Virol. **70:**341–351.
7. **Garnier, J., D. J. Osguthorpe, and B. Robson.** 1978. Analysis of the accuracy and implications of simple methods for predicting the secondary structure of globular proteins. J. Mol. Biol. **120:**97–120.
8. **Gascuel, O., and J. L. Golmard.** 1988. A simple method for predicting the secondary structure of globular proteins: implications and accuracy. Comput. Appl. Biosci. **4:**357–365.
9. **Gebhardt, A., J. V. Bosch, A. Ziemiecki, and R. R. Friis.** 1984. Rous sarcoma virus p19 and gp35 can be chemically crosslinked to high molecular weight complexes. J. Mol. Biol. **174:**297–317.
10. **Goff, S., P. Traktman, and D. Baltimore.** 1981. Isolation and properties of Moloney murine leukemia virus mutants: use of a rapid assay for release of virion reverse transcriptase. J. Virol. **38:**239–248.
11. **Gonzalez, S. A., J. L. Affranchino, H. R. Gelderblom, and A. Burny.** 1993. Assembly of the matrix protein of simian immunodeficiency virus into virus-like particles. Virology **194:**548–556.
12. **Granowitz, C., and S. P. Goff.** 1994. Substitution mutations affecting a small region of the Moloney murine leukemia virus MA gag protein block assembly and release of virion particles. Virology **205:**336–344.
13. **Hancock, J. F., H. Paterson, and C. J. Marshall.** 1990. A polybasic domain or palmitoylation is required in addition to the CAAX motif to localize $p21^{ras}$ to the plasma membrane. Cell **63:**133–139.
14. **Hansen, M., L. Jelinek, S. Whiting, and E. Barklis.** 1990. Transport and assembly of *gag* proteins into Moloney murine leukemia virus. J. Virol. **64:**5306–5316.
15. **Hockley, D. J., R. D. Wood, J. P. Jacobs, and A. J. Garrett.** 1988. Electron microscopy of human immunodeficiency virus. J. Gen. Virol. **69:**2455–2469.
16. **Hunter, E.** 1994. Macromolecular interactions in the assembly of HIV and other retroviruses. Sem. Virol. **5:**71–83.
17. **Jones, T. A., G. Blaug, M. Hansen, and E. Barklis.** 1990. Assembly of *gag*-β-galactosidase proteins into retrovirus particles. J. Virol. **64:**2265–2279.
18. **Jørgensen, E. C. B., F. S. Pedersen, and P. Jørgensen.** 1992. Matrix protein of Akv murine leukemia virus: genetic mapping of regions essential for particle formation. J. Virol. **66:**4479–4487.
19. **Kaplan, A. H., G. Mardon, J. M. Bishop, and H. E. Varmus.** 1988. The first seven amino acids encoded by the *v-src* oncogene act as a myristylation signal: lysine 7 is a critical determinant. Mol. Cell. Biol. **8:**2435–2441.
20. **Kim, J., T. Shishido, X. Jiang, A. Aderem, and S. McLaughlin.** 1994. Phosphorylation, high ionic strength, and calmodulin reverse the binding of MARCKS to phospholipid vesicles. J. Biol. Chem. **269:**28214–28219.
21. **Markowitz, D., S. Goff, and A. Bank.** 1988. A safe packaging line for gene transfer: separating viral genes on two different plasmids. J. Virol. **62:**1120–1124.
22. **Massiah, M. A., M. R. Starich, C. Paschall, M. F. Summers, A. M. Christensen, and W. I. Sundquist.** 1994. Three-dimensional structure of the human immunodeficiency virus type 1 matrix protein. J. Mol. Biol. **244:**198–223.
23. **Matthews, S., P. Barlow, J. Boyd, G. Barton, R. Russell, H. Mills, M. Cunningham, N. Meyers, N. Burns, N. Clark, S. Kingsman, A. Kingsman, and I. Campbell.** 1994. Structural similarity between the p17 matrix protein of HIV-1 and interferon-γ. Nature **370:**666–668.
24. **McLaughlin, S., and A. Anderem.** 1995. The myristoyl-electrostatic switch: a modulator of reversible protein-membrane interactions. Trends Biochem. Sci. **20:**272–276.
25. **Milligan, G., M. Parenti, and A. I. Magee.** 1995. The dynamic role of palmitoylation in signal transduction. Trends Biochem. Sci. **20:**181–186.
26. **Novotny, J., and C. Auffray.** 1984. A program for prediction of protein secondary structure from nucleotide sequence data: application to histocompatibility antigens. Nucleic Acids Res. **12:**243–255.
27. **Peitzsch, R. M., and S. McLaughlin.** 1993. Binding of acylated peptides and fatty acids to phospholipid vesicles: pertinence to myristoylated peptides. Biochemistry **32:**10436–10443.

28. **Pellman, D., E. A. Garber, F. R. Cross, and H. Hanafusa.** 1985. An N-terminal peptide from $p60^{src}$ can direct myristylation and plasma membrane localization when fused to heterologous proteins. Nature **314:**374–377.
29. **Perez, L. G., G. L. Davis, and E. Hunter.** 1987. Mutants of the Rous sarcoma virus envelope glycoprotein that lack the transmembrane anchor and cytoplasmic domains: analysis of intracellular transport and assembly into virions. J. Virol. **61:**2981–2988.
30. **Ragheb, J. A., and W. F. Anderson.** 1994. Uncoupled expression of Moloney murine leukemia virus envelope polypeptides SU and TM: a functional analysis of the role of TM domains in viral entry. J. Virol. **68:**3207–3219.
31. **Ragheb, J. A., and W. F. Anderson.** 1994. pH-independent murine leukemia virus ecotropic envelope-mediated cell fusion: implications for the role of the R peptide and p12E TM in viral entry. J. Virol. **68:**3220–3231.
32. **Rao, Z., A. S. Belyaev, E. Fry, P. Roy, I. M. Jones, and D. I. Stuart.** 1995. Crystal structure of SIV matrix antigen and implications for virus assembly. Nature **378:**743–747.
33. **Rein, A., M. R. McClure, N. R. Rice, R. B. Luftig, and A. M. Schultz.** 1986. Myristylation site in $Pr65^{gag}$ is essential for virus particle formation by Moloney murine leukemia virus. Proc. Natl. Acad. Sci. USA **83:**7246–7250.
34. **Rhee, S. S., and E. Hunter.** 1991. Amino acid substitutions within the matrix protein of type D retroviruses affect assembly, transport and membrane association of a capsid. EMBO J. **10:**535–546.
35. **Rost, B., and C. Sander.** 1993. Prediction of protein structure at better than 70% accuracy. J. Mol. Biol. **232:**584–599.
36. **Rost, B., and C. Sander.** 1994. Combining evolutionary information and neural networks to predict protein secondary structure. Proteins **19:**55–72.
37. **Schultz, A. M., L. E. Henderson, and S. Oroszlan.** 1988. Fatty acylation of proteins. Annu. Rev. Cell Biol. **4:**611–647.
38. **Schultz, A. M., and A. Rein.** 1989. Unmyristylated Moloney murine leukemia virus $Pr65^{gag}$ is excluded from virus assembly and maturation events. J. Virol. **63:**2370–2373.
39. **Shinnick, T. M., R. A. Lerner, and J. G. Sutcliffe.** 1981. Nucleotide sequence of Moloney murine leukemia virus. Nature **293:**543–548.
40. **Sigal, C. T., W. Zhou, C. A. Buser, S. McLaughlin, and M. D. Resh.** 1994. Amino-terminal basic residues of Src mediate membrane binding through electrostatic interaction with acidic phospholipids. Proc. Natl. Acad. Sci. USA **91:**12253–12257.
41. **Soneoka, Y., P. M. Cannon, E. E. Ramsdale, J. C. Griffiths, G. Romano, S. M. Kingsman, and A. J. Kingsman.** 1995. A transient three-plasmid expression system for the production of high titer retroviral vectors. Nucleic Acids Res. **23:**628–633.
42. **Spearman, P., J.-J. Wang, N. VanderHeyden, and L. Ratner.** 1994. Identification of human immunodeficiency virus type 1 Gag protein domains essential to membrane binding and particle assembly. J. Virol. **68:**3232–3242.
43. **Wedegaertner, P. B., P. T. Wilson, and H. R. Bourne.** 1995. Lipid modifications of trimeric G proteins. J. Biol. Chem. **270:**503–506.
44. **Wills, J. W., and R. C. Craven.** 1991. Form, function, and use of retroviral Gag proteins. AIDS **5:**639–654.
45. **Yu, X., X. Yuan, Z. Matsuda, T.-H. Lee, and M. Essex.** 1992. The matrix protein of human immunodeficiency virus type 1 is required for incorporation of viral envelope protein into mature virions. J. Virol. **66:**4966–4971.
46. **Yuan, X., X. Yu, T.-H. Lee, and M. Essex.** 1993. Mutations in the N-terminal region of human immunodeficiency virus type 1 matrix protein block intracellular transport of the Gag precursor. J. Virol. **67:**6387–6394.
47. **Zhou, W., L. J. Parent, J. W. Wills, and M. D. Resh.** 1994. Identification of a membrane-binding domain within the amino-terminal region of human immunodeficiency virus type 1 Gag protein which interacts with acidic phospholipids. J. Virol. **68:**2556–2569.